

Boron-modified Ordered Mesoporous Carbons as a novel electrode film for simultaneously Voltammetric Detection of Cadmium(II), Lead(II), Copper(II) and Mercury(II) ions

He-Lin Ye^{1,*}, Yan-ping Zheng¹, Rui Xue¹, Yu-Long Xie²

¹ School of Chemistry and Chemical Engineering, Lanzhou City University, Lanzhou 730070, China

² Key Laboratory of Resource Chemistry and Eco-environmental Protection in Tibetan Plateau of State Ethnic Affairs Commission, School of Chemistry and Chemical Engineering, Qinghai Nationalities University, Xining, Qinghai, 810007, China

*E-mail: yehelin82@163.com

Received: 3 September 2020 / Accepted: 30 October 2020 / Published: 31 January 2021

The boron-modified ordered mesoporous carbons (B-OMCs) was fabricated with controllable microstructure and ordered combination, used as a novel modified electrode film to detect trace amount of cadmium ion, lead ion, copper ion, and mercury ion. In this attribution, the detailed features of the B-OMCs modified electrode were studied. Four heavy metals were detected by using the method of cyclic voltammogram (CV) and differential pulse voltammetry (DPV). The prepared B-OMCs shows superior electrochemical activity, and it could be used for tracing cadmium ion, lead ion, copper ion, mercury ion simultaneously and selectively. The obtained results demonstrate the boron-modified carbon material broaden the potential applications, and therefore, the effect of Boron on the micro structure and electrochemical activity of OMC can be understood from the perspective of mechanism.

Keywords: boron-modified ordered mesoporous carbons, electrode, detect, cadmium ion, lead ion, copper ion, mercury ion.

1. INTRODUCTION

Due to the progress of science and technology and the development of economy, poisonous metal pollution cause a set of problems [1, 2], which not only pollutes the environment, but also endangers mankind's health. Heavy metal ions, for instance, cadmium ion, lead ion, copper ion, and mercury ion are poisonous and carcinogenic even in trace level of concentrations [3]. These heavy metal ions are non degradable and can be accumulated in living organs and tissues of humans and animals. Consequently, heavy metal ions can be supposed to one of the most principal contaminants for environmental water

and soil [4]. Heavy metals are usually discharged into the environment by various means [5] including vehicle emissions, mining business, battery manufacture, fossil fuel [6], metal electroplating and electronic industry. For detecting toxic heavy metal ions in complicated living environments, various techniques are involved to detect and analyze the ions such as complexometric titration, spectrophotometry, chemiluminescence [7], chromatography, electrochemical methods [8], spectroscopic methodology [9], mass spectrometry. Among these, electrochemical technique is a quick, convenient and low-priced mean to detect and remove toxic ions of heavy metals.

Along with the development of the electrochemistry, modification of electrodes surface with different materials has attracted substantial scientific interests. A number of modified electrodes have demonstrated superior performance in the determination of toxic pollutants, for example, gold nanoparticles [10], graphene composite material [11], carbon nanotubes [12], mesoporous silica [13], porous carbon materials and so on. Porous carbon materials, which are the traditional electrode materials that have been used over a long time. Due to a set of their exceptional characteristics, such as cheap, available, and excellent electrochemical stability [14–16], various types of carbon-based electrodes have aroused great concern. Porous carbon materials have the distinguishing characteristics of large specific surface area and pore volume, layered pore architecture, high mechanism and chemical stability, large adsorption capacities and good electric conductivity, etc, are also can be used as sensors for gas separation and water purification [17]. Among all kinds of porous carbon materials, ordered mesoporous carbon (OMC) has been paid more and more attention [18] because it can be further improved by periodically arranging uniform mesoporous space, customized pore size and optional pore shape [19]. Therefore, OMC has broaden the application prospects in energy conversion, adsorption, drug delivery and heterogeneous catalysis [20]. Although various modified OMC have been reported, there is still a need to develop novel materials to for precise heavy metal determination. In OMCs, the edge or end of carbon nanoplates are modified by a large number of active sites, which may be lattice defects or functional groups. Therefore, the chemical characteristics of OMC can be adjusted by functionalizing heteroatoms at the edges, defects or stress regions etc of graphene or carbon molecules. Up to now, people have been committed to the development of OMCs doped with heteroatoms (such as B [21], N [22], O [23], P [24], S [25]). The results indicate that the electronic properties of carbon can be adjusted, thus greatly improving the catalytic activity and electrochemical performance. Consequently, OMCs doped with heteroatom [26] have been considered to improve permeability of electrolyte and would be beneficial to enhance the electrochemical performance efficiently [27]. Compared to different heteroatoms involved, boron is a special element which contains trivalent electrons. The electronic structure has changed resulting from the reason that boron is doped in the carbon lattice and played a role as an electron acceptor, then the Fermi level guide band shift. As an advanced electrode material, boron doped carbon exhibit superior electrochemical characteristics [28]. Therefore, it is of great scientific significance to explore boron modified OMC with customizable microstructure and controllable proportion for revealing the electrochemical properties of the materials, broadening their potential application fields and in addition clarify the role of boron in its structure and activity.

In this paper, we explore a simple hydrothermal self-assembly and carbonization strategy to synthesize B-heteroatom OMCs, and discuss the chemical structures and electrochemical properties of electrode film. In conclusion, Boron / carbon source was needed as precursor and hard / soft template as

mesoporous forming agent for the synthesized process of boron modified OMC. In this work, boron rich OMCs were prepared by solvent evaporation induced self-assembly method, which can effectively synthesize OMCs with controllable multi-stage pore structure. The results show that the boron rich OMCs have controllable boron content, adjustable microstructure, excellent electrochemical sensitivity and rapidity.

Although B-modified mesoporous carbon has been tried using as a capacitor, it has not been used as electrode modifying film for the detection of heavy metal ions in water. Recently, the application of boron-rich carbon material to solve environmental problems has received considerable attention. Therefore, we prepared and characterized boron-rich OMCs, which was demonstrated to be utilized for the removal of cadmium ion, lead ion, copper ion, and mercury ion in such simple mode and sensitive, convenient treatment methods.

2. EXPERIMENTAL

2.1. Chemicals and instruments

All reagent were of analytical grade and can be used without further purification. 0.1M acetate buffer solution with pH 5.0 was prepared by mixing 0.1mNaAc and HAC stock solution. Water used in whole study process was double-distilled deionized.

An IviumStat electrochemical workstation were used to perform all electrochemical experiments. In this study, a standard three-electrode system was used, in which saturated calomel electrode (SCE) was adopted as reference electrode, while a platinum wire employed as the counter electrode and a bare or modified glassy carbon electrode (GCE) set as the working electrode. Transmission electron microscopy (TEM) (JSM-6500, JEOL Ltd., Tokyo, Japan) was use to characterize the morphologies of the samples. X-ray diffraction (XRD) on Rigaku D/MAX-2500 X-ray diffractometer with Cu K α irradiation ($\lambda=0.15406$ nm)was used to characterized the crystalline features.

2.2. Preparation of boron-modified ordered mesoporous carbons

21.0 g phenol, 22.0 g formaldehyde (37 wt%) and 3.75 g of 20 wt% sodium hydroxide (NaOH) aqueous solution mixed together in a flask at the temperature of 50°C, the temperature gradually increased to 75 °C and kept stirring for 1.0 h, then obtained a low-molecular-weight soluble phenolic resin. When the reaction finished, and until the mixture cooled down to room temperature, we used vacuum rotary evaporator to remove the water in the reaction system below 50 °C. After that, the water free mixture further react with 1.25 g boric acid and kept stirring for another 5.0 min, the resulting mixture was placed in a preheated oil bath and further stirred at 120 °C for 0.5 h, the newly formed water should be removed again by using vacuum rotary evaporator. With the help of ultrasonic equipment, the final product was dissolved in ethanol and the concentration of the solution was diluted to 30 wt%. Under these reacting conditions, finally obtained modified resol that was donated as B0.1-R, in which 0.1 means the ratio of boric acid to phenol.

Solvent evaporation induced self-assembly method [29] was applied to synthesize B0.1-OMC.

Through a classical preparing process, 20.0 g ethanol were used to dissolve 3.0 g F127 in the presence of 0.3 g HCl (37 wt%). Then slowly dripping 10.0 g B0.1-R (30 wt%) which previously get ready, and kept stirring for 0.5 h. Such homogeneous solution was poured into dishes, stay overnight to evaporated ethanol at room temperature, and then heat it in an oven at 100 °C for 24 h. The cured transparent film was scraped flattening, then heated in N₂ atmosphere at 350 °C for 2.0 h to remove the surfactant, and then carbonized at 800 °C for 2.0 h with a gradual change rate of 1.0 °C min⁻¹. The final product is represented as B0.1-OMC.

2.3. The Manufacture of electrochemical sensor

Before modifying the electrode, the exposed GCE was carefully rubbing down to mirror like surface using 0.3 and 0.05 mm alumina slurry respectively. After continuously ultrasonicate in ethanol and double distilled water, the electrode was repeatedly washed with double distilled water and dried at room temperature. The uniform black suspension was obtained by dispersing the B-OMCs materials into 0.05% Nafion aqueous solution via ultrasonication. After that, 5 μL of B-OMCs materials solution was dripped on the GCE pretreated and dried at the room temperature.

2.4. Measurements of Electrochemistry

Under optimized conditions, differential pulse anodic stripping voltammetric (DPASV) was employed for the detection. It presented higher anodic peak currents for Cd ion, Pb ion, Cu ion and Hg ion when choosing the scan rate of 25 mV·s⁻¹ [30]. The peak current increases with the increase of pulse amplitude, reaching to 100 mV. Therefore, the optimal parameters potential interval were -1.0 to +0.6 V (vs. SCE) for the simultaneous determination of Cd ion, Pb ion, Cu ion and Hg ion in samples by DPASV. The scanning rate was 25 mV · s⁻¹ and the pulse amplitude was 100 mV.

3. RESULTS AND DISCUSSION

The morphologies of boron-modified ordered mesoporous carbons was observed by TEM as shown in Fig. 1. From the low magnification TEM images, (Fig. 1a) the shows B-OMCs bears a considerable number of hole construction. From Fig. 1b we can see high-magnification TEM images, demonstrate that the sample was ordered architectures.

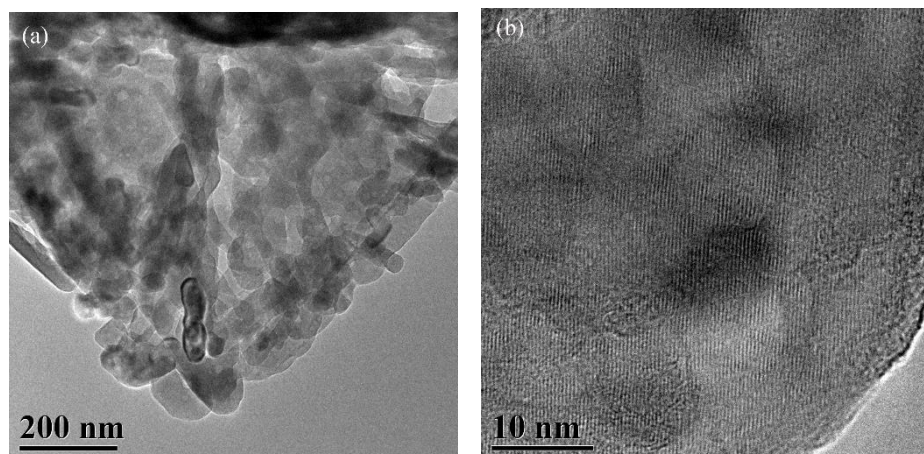


Figure 1. TEM images of B-OMCs.

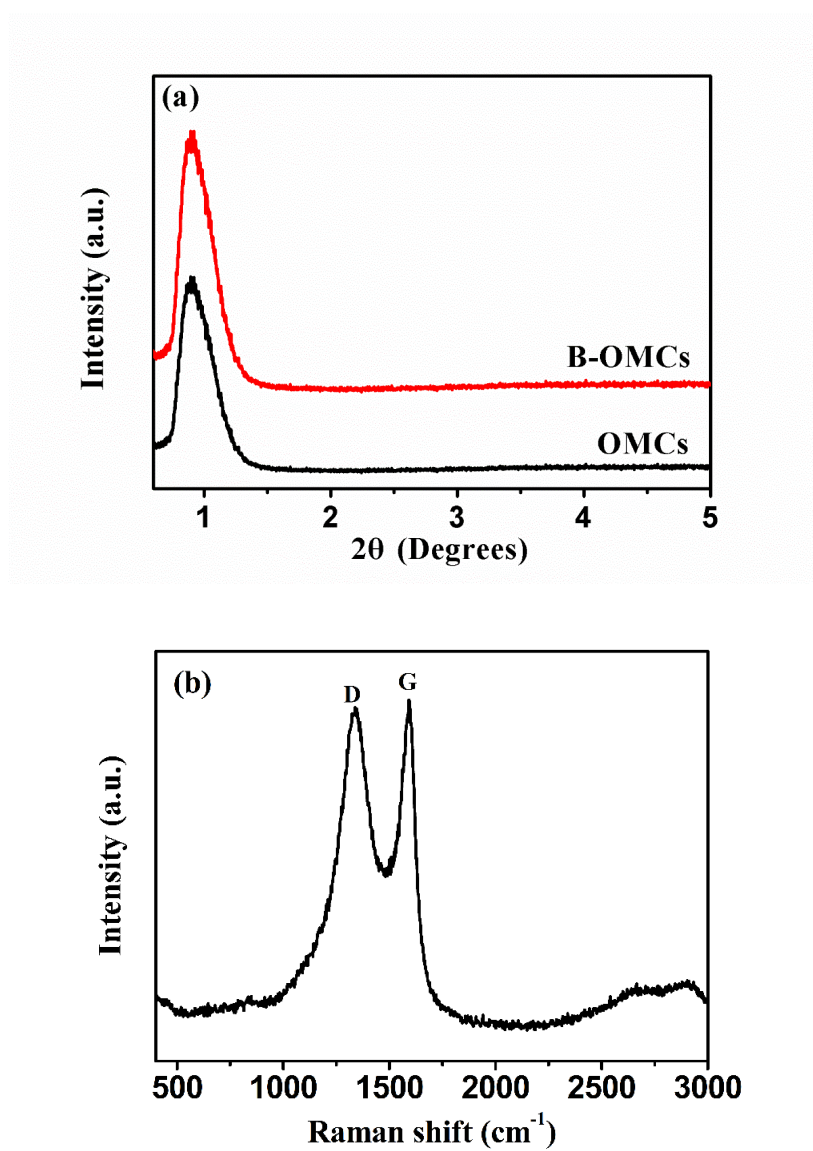


Figure 2. (a) XRD patterns for B-OMCs, and OMCs, (b) Raman spectrum of B-OMCs sample.

Low-angle XRD patterns for B-OMCs and OMCs were shown in Fig. 2a. There is an obvious diffraction peak near $2\theta = 1.0^\circ$, the strong peak of B-OMCs with center at $2\theta = 1.0^\circ$ can be considered as (100) reflection of 2D hexagonal ordered mesostructure[31]. indicating that the obtained boron-modified ordered mesoporous carbons possess a highly ordered mesoscopic structure over a large extent. In addition, compared with OMCs, B-OMCs shifted to the right slightly, indicating that B atoms were doped onto the OMCs. To characterize the microstructure of materials, Raman spectroscopy was also regarded as an effective method. As is shown in Fig. 2b, Raman tests were conducted in order to study the graphitization degree of B-OMC. The sample showed two evident peaks at 1346 and 1591 cm^{-1} , which respectively corresponded to D-band and G-band. Usually, the defect degree of graphite sheet was represented by the D-band, yet G-band related to the sp^2 hybrid conjugated structure. The I_D/I_G intensity ratio is commonly used as an indicator of measuring the graphitization degree [32]. The B-OMCs I_D/I_G intensity ratios of was 0.96 , implying that the sample is of higher graphitization degree, which is to advantage of improving its conductivity and promote the transition of electron into materials.

The DPASV analytical characteristics of naked GCE, OMCs, and B-OMCs modified GCE were presented in Fig. 3. When DPASV treatment was performed in a solution containing $1.0\ \mu\text{M}$, Cd ion, Pb ion, Cu ion, and Hg ion each of in $0.1\ \text{M}$ acetate buffer (pH 5.0) each exhibit a weak response at the naked GCE. There were also weaker peaks at the OMCs modified GCE which was observed from the potential range of -1.0 to $+0.6\ \text{V}$ (vs. SCE). unlikely from them, four objective metal ions showed higher and sharper peak currents on the B-OMCs electrode.

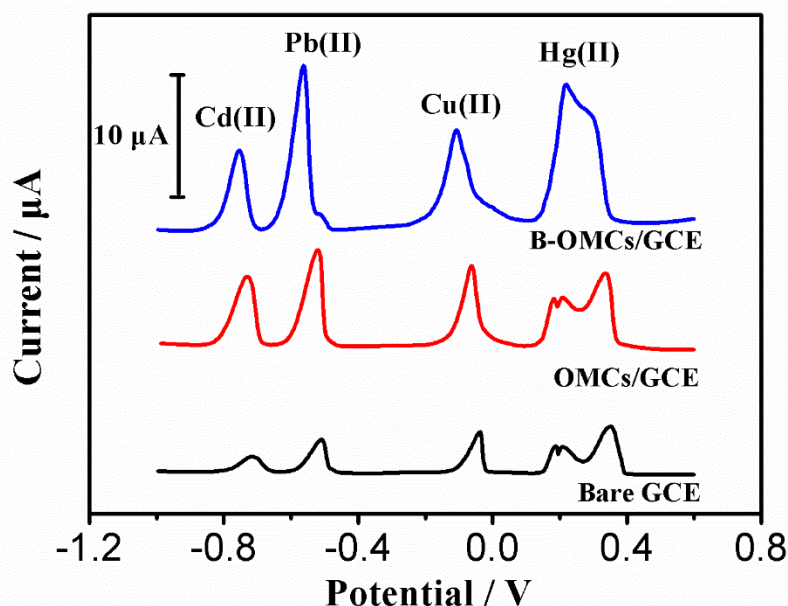


Figure 3. DPASV of $1.0\ \mu\text{M}$ Cd ion, Pb ion, Cu ion, and Hg ion on naked, OMCs, and B-OMCs modified GCE were compared in $0.1\ \text{M}$ acetate buffer (pH 5.0), vs. SCE.

Cd ion, Pb ion, Cu ion and Hg ion were simultaneously and individually determined by DPASV on the B-OMCs electrode under the optimum experimental conditions. The DPASV responses toward

Cd ion of different concentrations was shown in Fig. 4a. In the range of 0.01 to 1.5 μM , a clear peak proportional to the concentration of cadmium (II) was observed. Well-defined peaks, proportional to the concentration of Cd ion. Inset of Fig. 4a illustrate that the linear equation was $I (\mu\text{A}) = 1.36212 + 14.07863 C (\mu\text{M})$, and the correlation coefficients is 0.9988. The limit of detection (LOD) was determined to be 0.923×10^{-9} M (3σ method) by calculations. In the concentration range, the DPASV response of B-OMCs electrode to Pb ion ranged from 0.01 to 2.0 μM , as was shown in Fig. 5b. In the insert figure of Fig. 5b, it showed that the linear equation was $I (\mu\text{A}) = 2.81663 + 12.33483 C (\mu\text{M})$, and the correlation coefficient was 0.9963 and the LOD was 8.437×10^{-10} M (3σ method). Fig. 4c showed the DPASV responses of the B-OMCs electrode to Cu ion in the concentration range of 0.05 - 2.0 μM was shown in. Inset of Fig. 4c displayed that the linear equation was $I (\mu\text{A}) = 4.66958 + 10.21333 C (\mu\text{M})$, and the correlation coefficient of 0.9983 and LOD is 1.824×10^{-9} M (3σ method). Fig. 4d showed the DPASV responses of the B-OMCs electrode to Hg ion in the concentration range of 0.001 - 0.1 μM was shown in. Inset of Fig. 4d indicated that the corresponding linear equation was $I (\mu\text{A}) = 5.17178 + 62.33783 C (\mu\text{M})$, the correlation coefficient is 0.9973 and LOD is 2.046×10^{-10} M (3σ method). Therefore, B-OMCs electrode could be considered as an excellent platform for tracing and testing heavy metals.

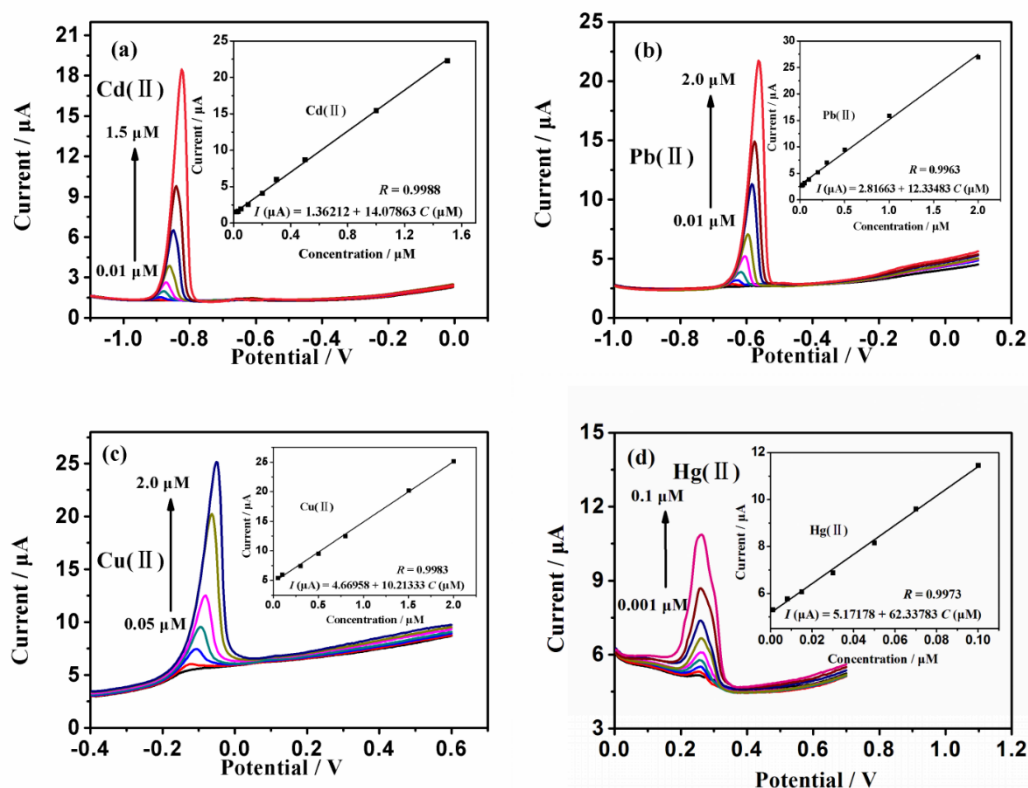


Figure 4. DPASV responses of the GCE modified by B-OMCs to (a) Cd ion in the concentration range of 0.02 to 1.5 μM , (b) Pb ion from 0.01 to 2.0 μM , (c) Cu ion from 0.05 to 2.0 μM , and (d) Hg ion from 0.001 to 0.1 μM .

Figure 5 showed typical DPASV analysis records for simultaneous analysis of Cd ion, Pb ion, Cu ion and Hg ion with the increasing concentrations by using B-OMCs electrode under optimal

experimental conditions. The prepared nanocomposite has been employed successfully to determine the four heavy metal ions simultaneously. For Cd ion, Pb ion, Cu ion, and Hg ion, there were individual peaks shown in their coexistence at around -0.73 , -0.52 , -0.06 , and 0.34 V vs. SCE, respectively. It is feasible to detect the four heavy metal ions simultaneously and selectively by using the B-OMCs electrode because the interval between the voltammetric peaks is large enough. The corresponding calibration curves for Cd(II) was established from $0.1 \mu\text{M}$ to $2.0 \mu\text{M}$, as is shown in Fig. 6a, while in inset of Fig. 6a, the linear equations were $I (\mu\text{A}) = 0.88935 + 8.77902 C (\mu\text{M})$, and the corresponding correlation coefficient is 0.9985 . By calculation, the limit of detection (LOD) was 1.475×10^{-9} M (3σ method).

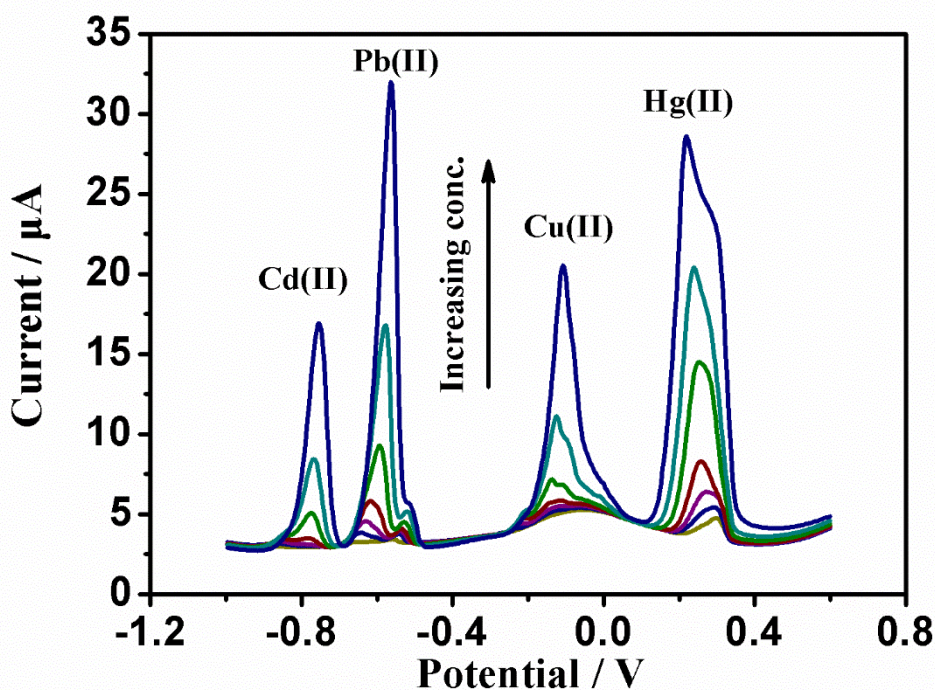


Figure 5. The simultaneous analysis of Cd ion, Pb ion, Cu ion, and Hg ion by the B-OMCs modified GCE(vs. SCE) for the DPASV response in a concentration range of 0.1 to $2.0 \mu\text{M}$,

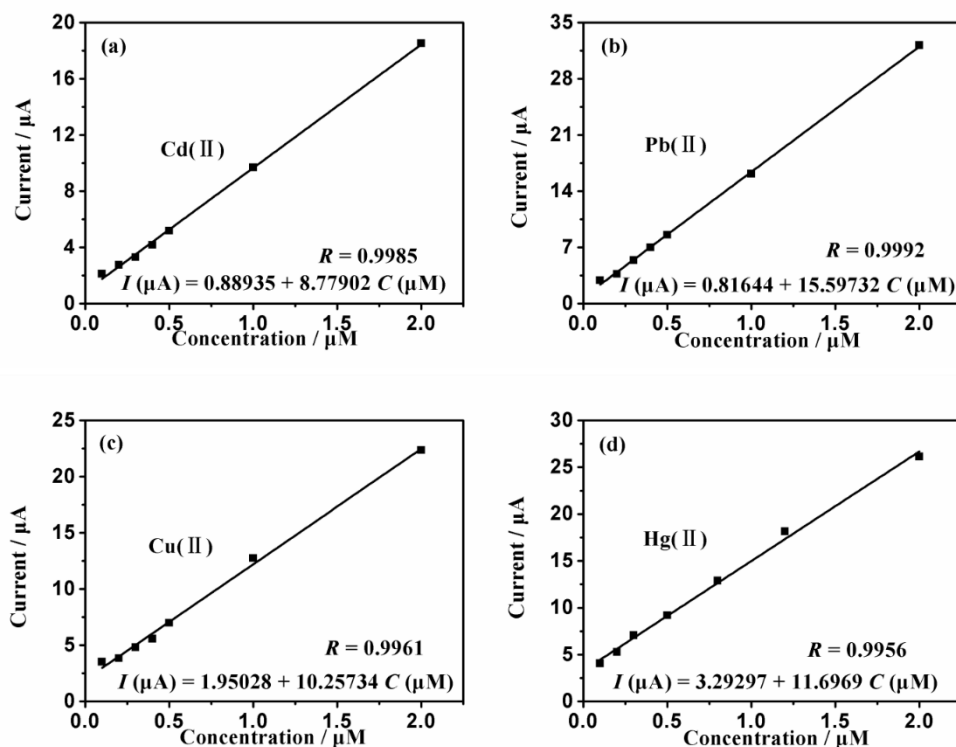


Figure 6. The calibration curves of Cd ion, Pb ion, Cu ion, and Hg ion corresponded to Figure 5.

The corresponding calibration curve of Pb(II) from 0.1 μM to 2.0 μM has been established as is shown in Fig. 6b, in the inset of Figure 6b, the linear equation was $I(\mu\text{A})=0.81644+15.59732 C(\mu\text{M})$, and the corresponding correlation coefficient was 0.9992, the calculated LOD value is 9.275×10^{-10} M (3σ method). The corresponding calibration curve for copper ions was established from 0.1 μM to 2.0 μM , as is shown in Figure 6c, the inset graph of Figure 6c indicate the linear equation was $I(\mu\text{A})=1.95028+10.25734c(\mu\text{M})$, and the corresponding correlation coefficient was 0.9961. The calculated LOD was 2.263×10^{-9} M (3σ method). Figure 6d, the LOD is calculated as 2.263×10^{-9} m (3σ method). The corresponding calibration curve was established for Hg(II) from 0.1 μM to 2.0 μM . The linear equation is $I(\mu\text{A})=3.29297+11.6969C(\mu\text{M})$, and the corresponding correlation coefficient is 0.9956 (Figure 6d inset). The LOD is calculated as 1.275×10^{-9} m (3σ method). As it is shown in Fig. 6d, the corresponding calibration curves for Hg(II) was established in the range of 0.1 μM to 2.0 μM . In the inset of Fig. 6d, the linear equation was $I(\mu\text{A}) = 3.29297 + 11.6969 C(\mu\text{M})$, the corresponding correlation coefficient was 0.9956. And the calculated LOD was 1.275×10^{-9} M (3σ method). The above calculated LOD values were much lower than the standard value offered by the World Health Organization (WHO).

In order to understand even better of the improvement of sensitivity, we further studied the effect of Cd ion or Pb ion concentration on the peak currents of Cu ion and Hg ion anode when analyzing Cu ion and Hg ion simultaneously. The DPASV responses of the B-OMCs electrode were revealed in Fig. 7a at different Cd ion concentrations when 2.0 μM Cu ion and 2.0 μM Hg ion were present in the solution, implying that there is interference of the Cd ion concentrations on the anodic peak currents of Cu(II) and

Hg(II). As can be seen from Fig. 7b, the peak current of Cu (II) increases slightly, when that of Hg (II) increases significantly with the addition of Cd ion. This result may be due to the formation of Cd film in the deposition step and then the Cd- Hg [33] intermetallic compounds were also formed in the process.

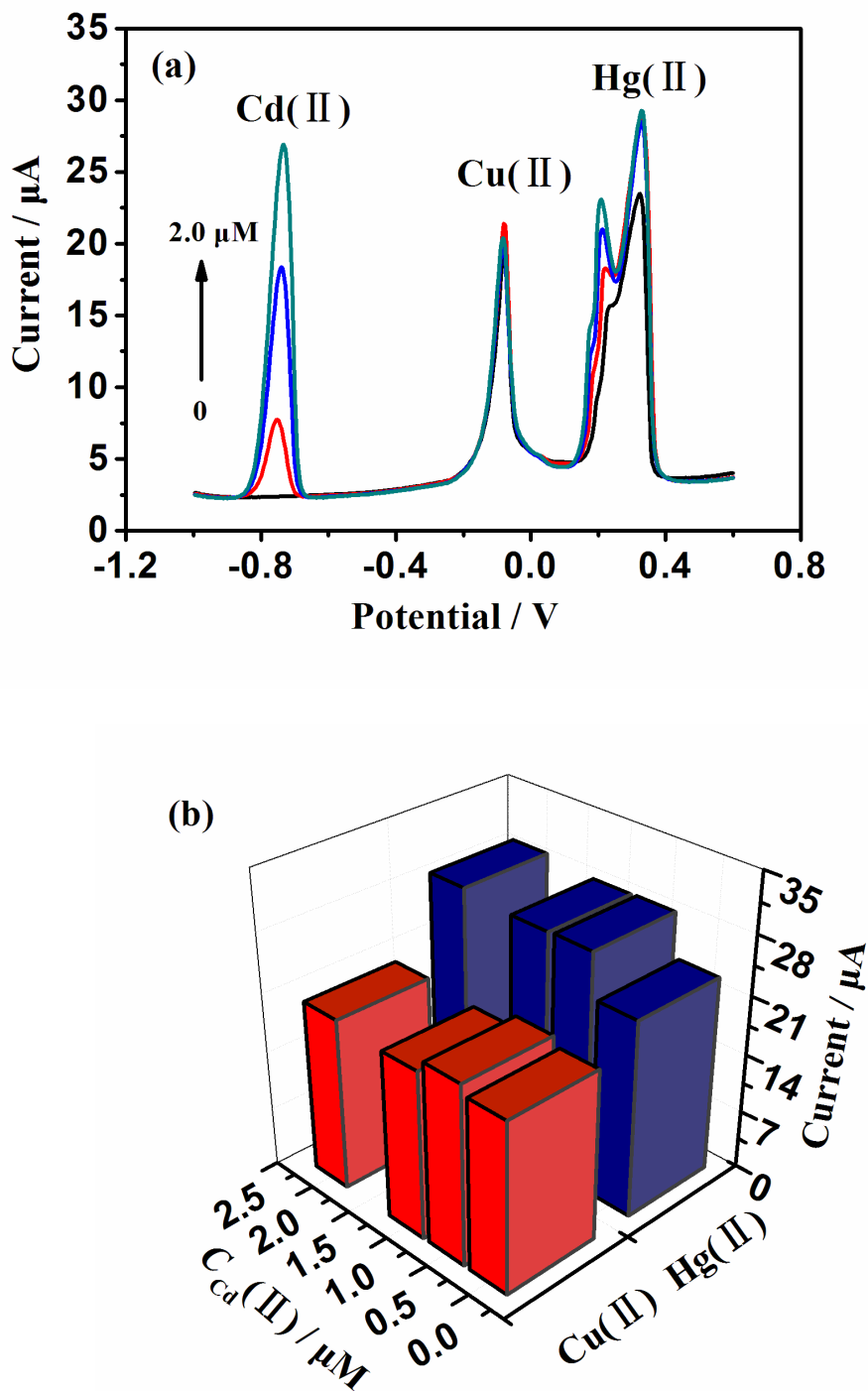


Figure 7. (a) The DPASV responses of GCE modified by B-OMCs at 0, 0.5, 1.0, and 2.0 μM Cd ion with the existence of 2.0 μM Cu ion and 2.0 μM Hg ion in 0.1 M NaAc-HAc (pH 5.0), indicating the Cd ion concentration interference that on the anodic peak currents of 2.0 μM Cu ion and 2.0 μM Hg ion. (b) At different Cd(II) concentrations, the comparison of the voltammetric peak current of Cu(II) and Hg(II) corresponding to panel a.

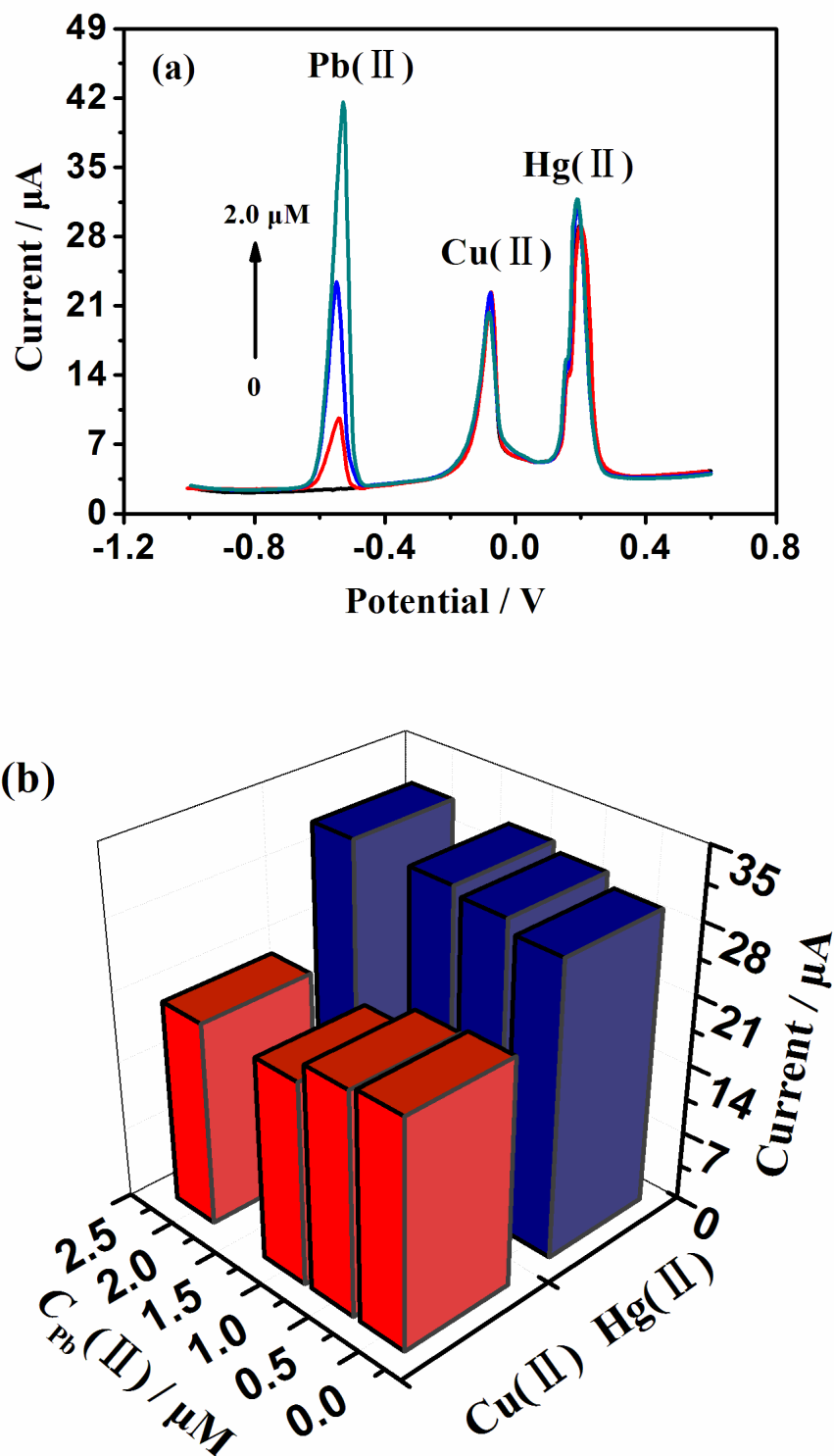


Figure 8. (a) with the existence of 2.0 μM Cu(II) and 2.0 μM Hg(II) in 0.1 M NaAc-HAc (pH 5.0), the DPASV responses of GCE modified by the B-OMCs at 0, 0.5, 1.0, and 2.0 μM Pb(II) indicating the Pb(II) concentrations interfered with the anodic peak current of 2.0 μM Cu(II) and 2.0 μM Hg(II). (b) At different Pb(II) concentrations, the comparison of the voltammetric peak current of Cu(II) and Hg(II) corresponding to panel a.

Similarly, the DPASV responses of the B-OMCs electrodes at different Pb ion concentrations with the existence of 2.0 μM Cu ion and 2.0 μM Hg ion were investigated. In Fig. 8, it showed that the peak currents of Cu ion and Hg ion increased slightly with Pb ion adding. Therefore, when it is measured at high concentrations of lead ion, a remarkable increase in analysis signals can be observed.

Herein, four target heavy metal ions can be simultaneously analyzed by the modified electrode. By investigating the influence of experiment conditions to achieve the electrochemical detecting optimization, Cd^{2+} , Pb^{2+} , Cu^{2+} , and Hg^{2+} can be detect at a low concentration simultaneously. In addition, the sensor had an outstanding performance and practical application value.

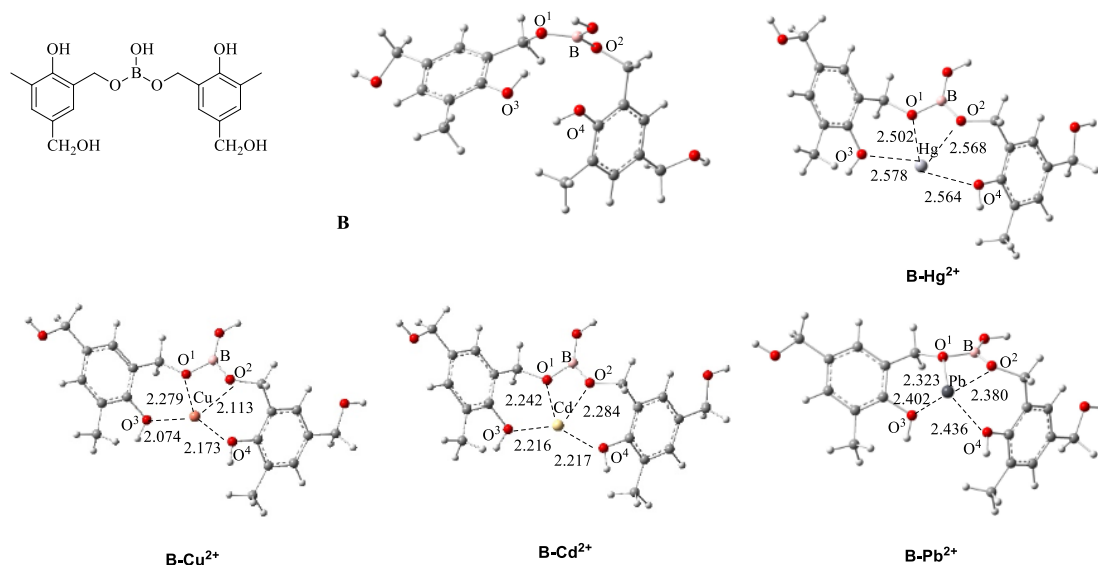


Figure 9. Chemical structure of boron-modified ordered mesoporous carbons and the heavy metals combining structures.

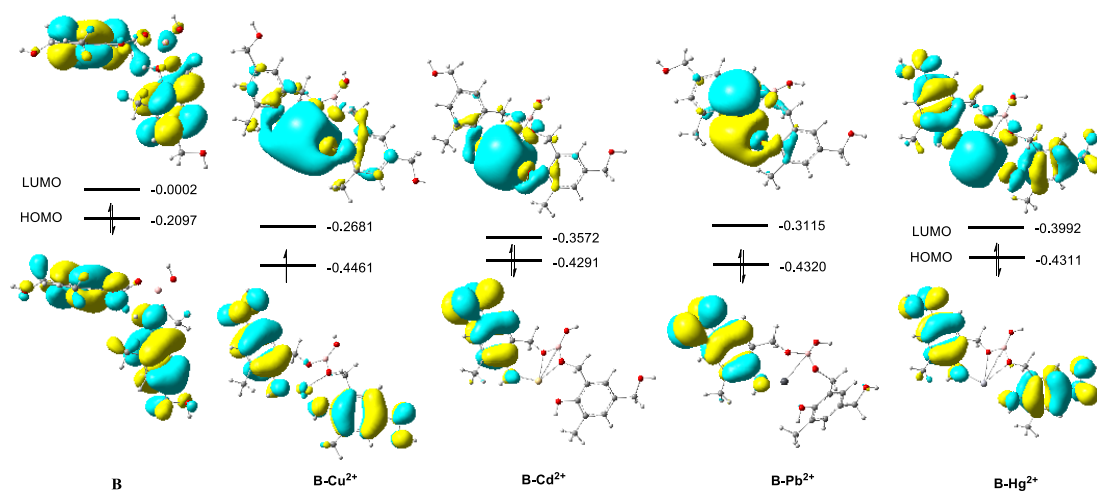


Figure 10. HOMO and LUMO molecular orbitals' isodensity diagram of boron-modified ordered mesoporous carbons and the heavy metals combining structures.

The chemical structures of boron-modified ordered mesoporous carbons and heavy metals

combining with boron-modified ordered mesoporous carbons structures were illustrated in Fig. 9. Firstly, Typical geometric parameters such as bond lengths of ground state geometrically optimized configuration were analyzed. Then, density functional theory (B3LYP) was used to optimize structure, the molecular orbitals were calculated from molecular orbitals with the same function and basis set [34]. For the reason that the relative positions of the occupied and virtual orbitals offered a reasonable qualitative instruction for the excitation properties and capabilities of electron or hole transportation, it is very helpful to study the highest occupied orbitals and the lowest virtual orbitals of these molecules. Since the first dipole allowed for electron transitions, that means, the strongest electron transitions with the largest oscillator strength, it almost completely corresponds to the promotion of electrons from the highest occupied molecular orbital (HOMO) to the lowest unoccupied molecular orbital (LUMO). The HOMO and LUMO molecular were plotted in Fig. 10. The frontier orbitals of these molecules were distributed in the whole p-conjugated main chain. Generally speaking, HOMO had anti-bonding property between subunits. The other side of the shield, LUMO of all the molecules usually exhibit a bonding property between the subunits [35]. This means that the singlet excited state mainly involving electrons from HOMO to the LUMO should be more planar. As is known to all that the energy of the band gap (E_{gap}) between HOMO and LUMO energies is an important parameter to determine the molecular admittance. Thus, the electronic properties mainly relied on HOMO, LUMO energy levels, and the electron hole migration rate.

The B atom activates the oxygen activity in the mesoporous carbon due to its electron-deficient properties, the d-vacancy orbital of transition metal ion interacts with the non-bonding electrons of oxygen atom. Such situation enabled the boron-modified mesoporous carbon can be used as a sensitive electrode for detecting heavy metal ions.

4. CONCLUSIONS

A new type of porous B-OMCs with high surface area and B doped has been fabricated successfully using a solvent evaporation induced self-assembly method. This material can be used to develop a modified electrode for determining the Cd ion, Pb ion, Cu ion and Hg ion simultaneously. The elaborated B-OMCs offered the B doped network which could facilitate the penetration and rapid electron transmission. The synthetic material is a promising electrochemical testing material for heavy metal ions, and furthermore was sensitive electrode for the analysis of Cd (II), Pb (II), Cu (II) and Hg (II) by DPASV with satisfactory results. The LOD obtained in the experiment is much lower than the World Health Organization (WHO) guidelines, which means that the method is practical and feasible in aqueous solution or wastewater with approving results. Optimized structures and quantum chemical calculations proved that the B-OMCs exhibit excellent conductivity performance. In summary, this work would broaden a new way to design and synthesize porous B modified carbon materials and could be applied in electrochemical and environmental fields.

Declaration of Conflicting Interests

The authors declare no conflict of interest.

ACKNOWLEDGEMENTS

This work was financially supported by Innovation ability improvement program of colleges and Universities of Gansu province (No.2020B-233) and Teacher Doctoral Research Start-Up Funding of Lanzhou City University (LZCU-BS2015-09). Also supported from the Research Program of Application Foundation of Qinghai Province (No. 2019-ZJ-7013), Chunhui Project of the Ministry of Education (Z2017044).

References

1. L. Joseph, B. M. Jun, J. R. V. Flora, C. M. Park, Y. Yoon, *J. Chemosphere*, 229 (2019) 142.
2. M. d'Halluin, J. Rull-Barrull, G. Bretel, C. Labrugère, E. L. Grogneq, F.-X. Felpin, *ACS Sustain. Chem. Eng.*, 5 (2017) 1965.
3. X. Wei, X. Kong, S. Wang, H. Xiang, J. Wang, J. Chen, *Ind. Eng. Chem. Res.*, 52 (2013) 17583.
4. F. Iemma, G. Crillo, U. G. Sipizzirri, F. Puoci, O. I. Parisi, N. Picci, *Europ. Polym. J.*, 44 (2008) 1183.
5. A. Denizli, B. Garipcan, A. Karabakan, H. Senöz, *Materials Science & Engineering C*, 25 (2005) 448.
6. M. D. Machado, E.V. Soares, H. M. Soares, *J. Hazard. Mater.*, 184 (2010) 357.
7. J. Paul Chen, L. L. Lim, *Chemosphere*, 60 (2005) 1384.
8. Y. Wan, X. Wang, S. Liu, Y. Li, H. Sun, Q. Wang, *Int. J. Electrochem. Sci.* 8 (2013) 12837.
9. S. Niu, L. J. Zheng, A. Q. Khan, G. Feng, H. P. Zeng, *Talanta*, 179 (2018) 312.
10. X. Xu, G. Duan, Y. Li, G. Liu, J. Wang, H. Zhang, Z. Dai, W. Cai, *ACS Appl. Mater. Interf.*, 6 (2014) 65.
11. Y. Wei, C. Gao, F. L. Meng, H. H. Li, L. Wang, J. H. Liu, X. J. Huang, *J. Phys. Chem. C.*, 116 (2012) 1034.
12. B. C. Janegitz, L. C. S. Figueiredo-Filho, L. H. Marcolino-Junior, S. P. N. Souza, E. R. Pereira-Filho, O. Fatibello-Filho, *J. Electroanal. Chem.*, 660 (2011) 209.
13. W. Yantasee, Y. Lin, G. E. Fryxell, B. J. Busche, *Anal. Chim. Acta*, 502 (2004) 207.
14. D. S. Su, R. Schlögl, *ChemSusChem.*, 3 (2010) 136.
15. C. D. Liang, Z. J. Li, and S. Dai, *Angew. Chem. Int. Ed.*, 47 (2008) 3696.
16. Y. H. Zhang, A. Q. Wang and T. Zhang, *Chem. Commun.*, 46 (2010) 862.
17. J. Lee, J. Kim, T. Hyeon, *Adv. Mater.*, 18 (2006) 2073.
18. Alain Walcarius, *Sensors*, 17 (2017) 1863.
19. W. X. Liu, N. Liu, H. H. Song, X. H. Chen, *New Carbon Materials*, 26 (2011) 217.
20. Y. F. Shi, Y. Wan and D. Y. Zhao, *Chem. Soc. Rev.*, 40 (2011) 3854.
21. D. Portehault, C. Giordano, C. Gervais, I. Senkowska, S. Kaskel, C. Sanchez and M. Antonietti, *Adv. Funct. Mater.*, 20 (2010) 1827.
22. T. Kwon, H. Nishihara, H. Itoi, Q. H. Yang and T. Kyotani, *Langmuir*, 25 (2009) 11961.
23. C. Moreno-Castilla, M. B. Dawidziuk, F. Carrasco-Marin and Z. Zapata-Bennabithé, *Carbon*, 49 (2011) 3808.
24. P. Mohanty and K. Landskron, *J. Mater. Chem.*, 19 (2009) 2400.
25. G. Hasegawa, M. Aoki, K. Kanamori, K. Nakanishi, T. Hanada, K. Tadanaga, *J. Mater. Chem.*, 21(2011) 2060.
26. D. W. Wang, F. Li, Z. G. Chen, G. Q. Lu and H. M. Cheng, *Chem. Mater.*, 20 (2008) 7195.
27. T. Morita and N. Takami, *Electrochim. Acta*, 49 (2004) 2591.
28. X. C. Zhao, A. Q. Wang, J. W. Yan, G. Q. Sun, L. X. Sun and T. Zhang, *Chem. Mater.*, 22 (2010) 5463.
29. X.C. Zhao, Q. Zhang, B.S. Zhang, C.M. Chen, J. M. Xu, A.Q. Wang, D. S. Su and T. Zhang, *RSC Adv.*, 3 (2013) 3578.

30. Y. L. Xie, S. Q. Zhao, H. L. Ye, J. Yuan, P. Song, S. Q. Hu, *J. Electroanal. Chem.*, 757 (2015) 235.
31. G. Zhao, H. Wang, G Liu, and Z.q. Wang, *Electroanalysis*, 29(2017) 497.
32. M. Wu, Y. Li, B. Yao, J. Chen, C. Li, G. Shi, *J. Mater. Chem. A.*, 4 (2016) 16213.
33. J. Schiewe, K. B. Oldham, J. C. Myland, A. M. Bond, V. A. Vicente-Beckett, S. Fletcher, *Anal. Chem.*, 69 (1997) 2673.
34. S.Q. Zhao, Y. L. Xie, Z. X. Qi, P. C. Lin, *Int. J. Electrochem. Sci.*, 13 (2018)1945.
35. M.Abd El-Raouf, E.A.Khmis, M.T.H.Abou Kana, and N.A.Negm, *J.Mol.liq.*, 255 (2108) 341.

© 2021 The Authors. Published by ESG (www.electrochemsci.org). This article is an open access article distributed under the terms and conditions of the Creative Commons Attribution license (<http://creativecommons.org/licenses/by/4.0/>).